High Efficiency Ceramic Lasers

J.S. Sanghera, W. Kim, C. Baker, G. Villalobos, J. Frantz, L.B. Shaw, A. Lutz, and I. Aggarwal
Optical Sciences Division

The Problem: Lightweight and compact high power lasers will facilitate integration of directed energy weapons systems on board tactical platforms without compromising mobility (Fig. 1). Solid-state crystal lasers would be ideal for these applications. Single-crystal yttrium aluminum garnet (YAG) has been the workhorse of solid-state crystal lasers, whereby doping YAG with about 1% to 2% of rare earth ions (e.g., Yb^{3+}

FIGURE 1
Schematic representation of terrestrial and airborne platforms with high energy laser systems.

or Nd^{3+}) has led to lasing at a wavelength of ~1 μm. However, scaling to very high laser powers with good beam quality in YAG is limited by its thermal conductivity and the sudden drop in thermal conductivity with increasing dopant concentration. An additional problem is the poor dopant solubility in YAG, which leads to non-uniform dopant concentration, a big problem at high dopant concentrations. A better solution is to use materials with better dopant solubility and higher thermal conductivity, such as the sesquioxide Lu_2O_3. In fact, the thermal conductivity for Lu_2O_3 remains relatively constant with increasing dopant concentration due to the similarity of the phonon energy of the dopant and the host. However, single-crystal Lu_2O_3 is difficult to make by traditional high-temperature crystal growing from the melt, due its very high melting temperature of 2400 °C. This leads to crucible reactions, volatilization, chemical inhomogeneity, lattice strain, defects, and cracks, which therefore limit the size of the crystal to the millimeter scale. These small sizes are not suitable for making high power lasers. Therefore, alternative methods are needed to make suitable-sized solid-state laser materials.

The Solution: The polycrystalline ceramic process is a method that can mitigate the problems associated with growing single crystals from their melts at high temperature. This process uses high-purity, submicron powder that is densified at only two-thirds of the melt temperature using vacuum sintering or hot pressing. The small size of the powder makes it very accommodating to lattice strain and so it is easy to dope with high levels of rare earth ions. Also, the product is a polycrystalline material, typified by grains and grain boundaries. The grains, which are single crystals, can range in size from a few microns to several tens of microns. As their size is small, they can also accommodate higher rar earth ion dopant concentration, with any additional lattice strain being accommodated by the grain boundaries. If the grain boundaries are clean, i.e., without impurities, then the polycrystalline ceramic will be transparent and with high optical quality. This process is readily scalable to large sizes and conformal shapes. A further advantage is that ceramics are tougher and stronger than their crystalline counterparts and so they possess a higher threshold for thermal shock, thereby enabling higher laser output power.

Experimental Details and Results: We have developed wet chemistry processes to make submicron Yb^{3+}:Lu_2O_3 powder that has a particle size of approximately 100 nm, surface area of 33 m^2/g and less than 1 ppm impurity content. The powder is uniformly doped with tailored amounts of the dopant Yb^{3+}. Hot pressing this fine, non-agglomerated powder at ~1600 °C for a couple of hours under a load of ~5,000 psi

FIGURE 2
A polished 1-in.-diameter transparent 10% Yb^{3+} doped Lu_2O_3 ceramic sample.

yields a partially transparent ceramic with >99% density. Subsequent hot isostatic pressing (HIP) at ~1600 °C using an argon gas pressure of 30,000 psi completes the process by increasing the density to 100% and providing full transparency. Figure 2 shows a polished 1-in.-diameter transparent 10% Yb^{3+} doped Lu_2O_3 ceramic sample that exhibits excellent optical quality. Pumping this sample with a diode laser operating at 975 nm leads to lasing with more than 16 W output power at 1080 nm and a slope efficiency of 74% (Fig. 3). This result represents the highest output power and highest efficiency obtained from Lu_2O_3 ceramics. What makes this result even more remarkable is the high doping concentration of 10% Yb^{3+}. This technology, along with several patents, has been licensed to industry. The domestic availability of transparent rare-earth-doped Lu_2O_3 ceramics will enable fabrication of ceramic laser materials for power scaling and implementation in highly efficient and compact directed energy weapons systems.

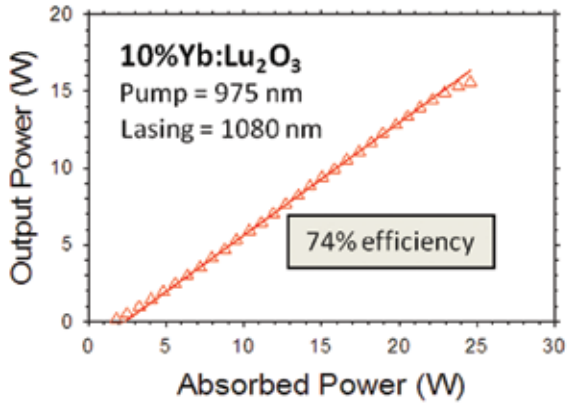

FIGURE 3
Output laser power at 1080 nm vs absorbed pump laser power at 975 nm.

Acknowledgments: The authors would like to acknowledge the financial support provided by the Joint Technology Office for High Energy Lasers (JTO-HEL) and the Office of Naval Research (ONR) as well as the efforts of Michael Hunt (University Research Foundation), and Bryan Sadowski and Fritz Miklos (Global Defense Technology & Systems, Inc.).

[Sponsored by NRL/ONR and JTO-HEL]

Aerosol Agent Detection Using Spectroscopic Characterization

V. Sivaprakasam,[1] J. Czege,[2] M. Currie,[1] J. Lou,[2] and J. Eversole[1]
[1]*Optical Sciences Division*
[2]*Global Defense Technology & Systems, Inc.*

Introduction: Detection of chemical and biological agents that would most likely be dispersed as aerosols has become a critical component of modern defense capability. Under a Defense Threat Reduction Agency (DTRA) supported program, the NRL Optical Sciences Division has recently developed advanced ambient air monitoring and aerosol classification technologies based on laser interrogation and spectroscopy. These optical characterization measurements are performed on individual aerosol particles entrained in a continuous air stream as they move past the sensor focal volume at rates up to 10,000 per second. Multiple laser beams at several wavelengths are used to interrogate the particles. Six beams are generated by one continuous-wave visible wavelength diode laser and collectively provide position and velocity information of the aerosol particles. Subsequently, each particle is illuminated with one or two pulsed ultraviolet (UV) lasers. If the particle is composed of biological material, the UV lasers will excite characteristic fluorescence. These UV laser-induced fluorescence (UV-LIF) signals from discrete spectral channels are recorded, as are the elastic scattering intensities. Up to 14 optical measurements may be obtained from each particle. These data values are used to differentiate and classify the particles into potential-threat or non-threat categories.

Spectral Discrimination: Figure 4 shows a scatter plot survey of UV-LIF particle signatures from eight separate populations with different compositions as described in the legend and elsewhere.[1] The data shown are the sum of the emission intensities from multiple channels for the two indicated excitation wavelengths. The aerosol particles shown here are approximately one micron in diameter, and each point on the plot represents a single particle. One can easily see that significant discrimination is obtained for four broad categories of different materials, including those relevant to biological agents. However, the spread in these particle data includes variation in instrument optical collection efficiency and laser illumination of the particle depending on its location in the sensor focal volume. To improve discrimination, we have implemented a new laser beam design to reduce variability due to particle position.

Instrument Design: The basic optical design has been previously published,[1] and contains greater detail than can be accommodated here. The original design uses a single separate continuous-wave laser beam as a "trigger" to indicate the presence of an aerosol particle entering the instrument, and cue the firing of pulsed UV lasers. Most recently, this trigger beam has been split into a set of six spatially structured beams that provide data on the specific position and velocity of each particle. This arrangement, referred to as

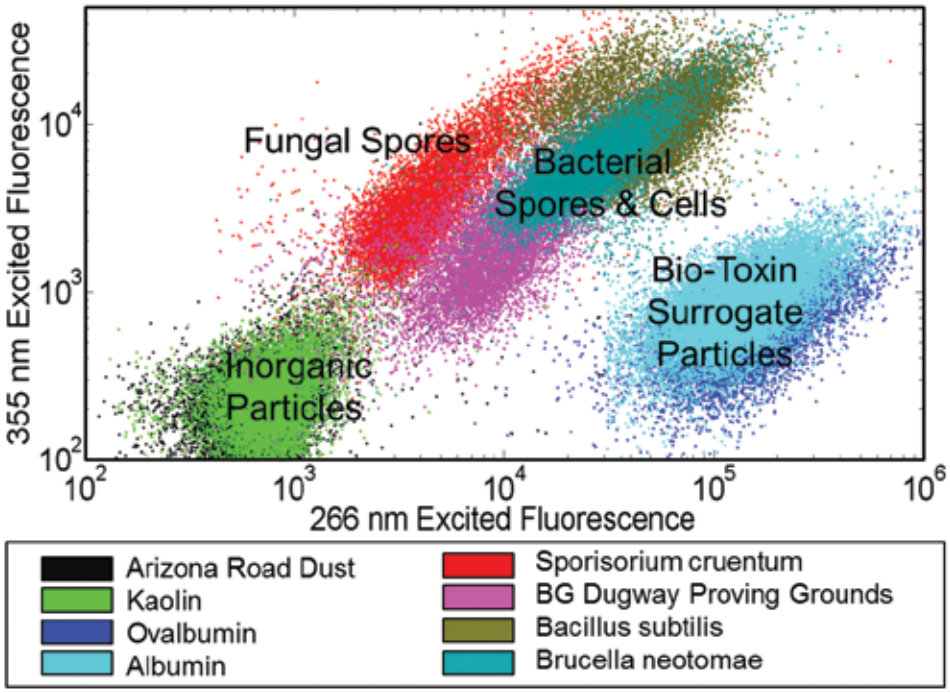

FIGURE 4
An illustration of the separation observed in measured UV-LIF emission intensities in two spectral channels from lab-generated populations of aerosol particles representing four broad groups: inorganic ambient background particles, fungal spores, bacterial particles (spores or cells), and bio-toxin surrogates (proteins). The eight specific example compositions are color-coded in the legend.

a structured trigger beam (STB),[2] provides the ability to reduce the spread of the fluorescence and elastic scattering data used to characterize the particle. By knowing the precise particle location, the instrument response function due to spatially dependent laser beam intensity profiles and optical collection efficiency can be normalized. Figure 5 shows the precision mask (a) used to generate six spatially distinct STB laser beams, and a typical oscilloscope trace (b) of a particle passing through these beams (lower, blue trace). The particle position and velocity is coded into the relative positions of these six pulses generated by the particle passing through each beam. Figure 5(c) shows typical x-y-z trajectories for an ensemble of particles calculated from the STB data, while Fig. 5(d) shows the (parabolic) distribution of flow velocities for the same particles as a function of their position (x-y) in the flow cross section. Finally, the effectiveness of the STB positional data to normalize fluorescence intensities can be seen by comparing Fig. 5(e) to Fig. 5(f). Figure 5(e) shows a histogram of un-normalized (raw) fluorescence pulse heights, while Fig. 5(f) shows the same data normalized for spatial position instrument response. The result clearly shows the presence of three distinct test populations of fluorescent particles that were previously completely obscured.

Future Directions: In the past year, we have also developed customized UV laser light sources that offer certain advantages, such as greater energy efficiency, over the commercially available laser systems employed so far (e.g., 266 and 355 nm wavelength lasers). Figure 6(a) shows a photograph of an NRL-developed, mode-locked fiber laser that provides high-intensity pulses (<500 fs in duration) at a 41 MHz repetition rate.[3] The photograph shows the coiled optical fiber laser (as bright purple) as well as its second harmonic converted light (as green). The fiber laser pulse intensities are sufficiently high that two-photon absorption can be used to effectively produce fluorescence. The scatter plot in Fig. 6(b) shows UV fluorescence intensities in two spectral bands from three different populations of aerosol particles excited by green laser light. These data are the first published[3] observations of emission due to multiphoton absorption from bacterial aerosol particles.

[Sponsored by DTRA]

References

[1] V. Sivaprakasam, A. Huston, C. Scotto, and J. Eversole, "Multiple UV Wavelength Excitation and Fluorescence of Bioaerosols," *Opt. Express* **12**, 4457–4466 (2004); V. Sivaprakasam, H.-B. Lin, A.L. Huston, and J.D. Eversole, "Spectral Characterization of Biological Aerosol Particles Using Two-Wavelength Excited Laser-Induced Fluorescence and Elastic Scattering Measurements," *Optics Express* **19**(7), 6191–6208 (2011).

[2] W.D. Herzog, S.M. Tysk, D.W. Tardiff, G.C. Cappiello, J.M. Jong, T.H. Jeys, R.H. Hoffeld, A. Sanchez, and V. Daneu, "Measurement of Aerosol Particle Trajectories Using a Structured Laser Beam," *Appl. Opt.* **46**, 3150–3155 (2007).

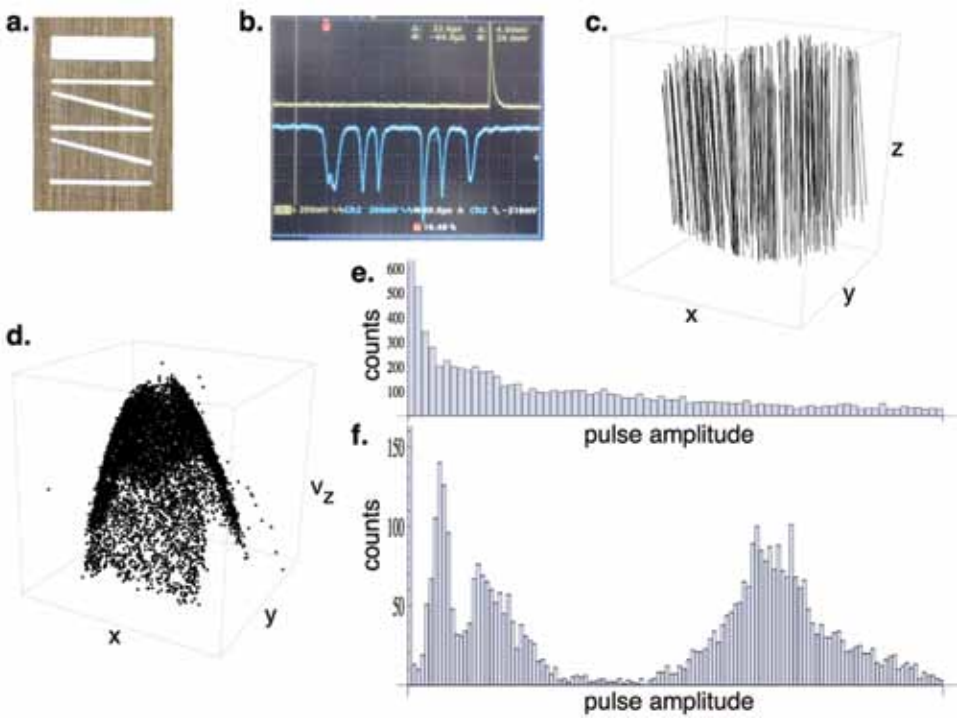

FIGURE 5
Different aspects of the structured trigger beam (STB) are shown, starting with: (a) the high-precision mask used to generate the six beams, (b) a typical oscilloscope trace (blue trace) showing the six-pulse signature as a particle passes through each of the beams, (c) a three-dimensional representation of particle trajectories for an ensemble of particles created from STB data, (d) the corresponding velocity (v_z) profile from that particle ensemble, (e) uncorrected LIF pulse height data from test particles, and (f) the same LIF data as in (e), corrected now using the STB data, and revealing the presence of three distinct fluorescent populations.

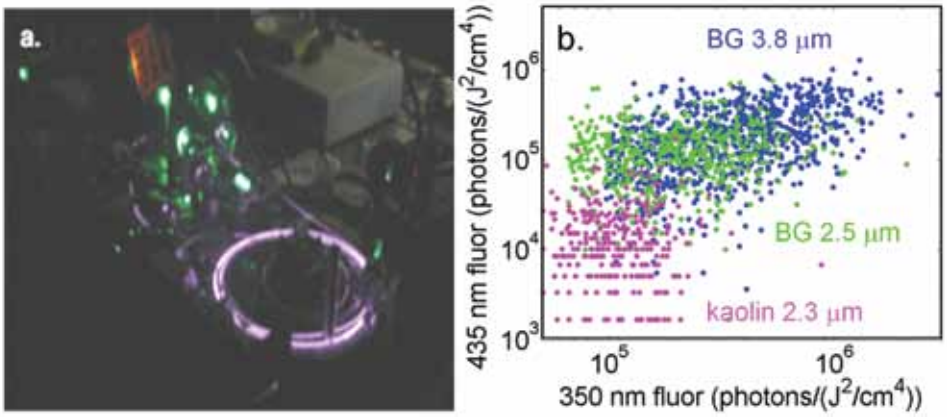

FIGURE 6
(a) A photograph of a unique, mode-locked fiber laser developed to provide a continuous train of short (<500 fs) pulses of light for aerosol particle interrogation. The laser fundamental wavelength can be either doubled to 526 nm (green) or quadrupled to 263 nm (UV) very efficiently. (b) Because of its high peak power, two-photon absorption of the laser green light results in UV fluorescence from aerosol particles of bacterial spores (BG clusters of 2.5 and 3.8 μm diameters) compared to nonfluorescent mineral particles (kaolin) of similar size as shown in this scatter plot.

[3] J.W. Lou, M. Currie, V. Sivaprakasam, and J.D. Eversole, "Green and Ultraviolet Pulse Generation with a Compact, Fiber Laser, Chirped-Pulse Amplification System for Aerosol Fluorescence Measurements," *Rev. Sci. Instrum.* **81**(10), 103107 (2010); V. Sivaprakasam, J. Lou, M. Currie, and J.D. Eversole, "Two-Photon Excited Fluorescence from Biological Aerosol Particles," *JQSRT* **112**(10), 1511–1517 (2011).

Angel Fire/Blue Devil Sensors for Wide-Area ISR and Persistent Surveillance

J.N. Lee, M.R. Kruer, D.C. Linne von Berg, J.G. Howard, B. Daniel, and P. Lebow
Optical Sciences Division

Introduction: The Applied Optics Branch has been developing technology for use in a broad range of tactical and wide-area surveillance systems. These systems include high-resolution, high-framing-rate, panchromatic, and hyperspectral imaging systems in the visible through infrared spectral regions, on platforms ranging from low-altitude small UAVs to high-altitude standoff aircraft. Recently, a dual-band wide-area persistent surveillance sensor system (DB-WAPSS) has been developed, flight-tested, and transitioned. The DP-WAPSS IR subsystem uses a 16.7-megapixel mid-wave infrared (MWIR) focal plane array (FPA; 4096 × 4096 pixel, 15-μm pixel pitch, sensitive from 3.5 to 5.1 μm wavelength) to provide the largest presently available day/night IR coverage in addition to increased resolution performance at lower altitudes. The visible subsystem is a large-format 59-megapixel camera that can operate at high frame rates. Both imaging subsystems are incorporated into a step-stare gimbal, the CA-247 from Goodrich ISR Corporation, that can increase coverage by creating a mosaic of images, i.e., trading update rate against area coverage. The DB-WAPSS/CA-247 system has been demonstrated to a Technology Readiness Level (TRL)-7 level of maturity, showing direct application to existing and developing wide-area persistent surveillance airborne platforms used by U.S. Navy, U.S. Marine Corps, U.S. Air Force, and U.S. Army. Seven sensors were developed for the Marine Corps' Angel Fire program, each sensor showing high-level, reproducible performance; these sensors have since transitioned to other Services' applications, in particular the Air Force's Blue Devil program. We describe key subsystem breakthroughs and resultant system performance.

Focal Plane Array and Sensor Development: Major challenges for focal planes for framing-camera applications are maximizing the number of pixels per array and simultaneously maximizing the array frame rate. Silicon FPAs for the visible/near-IR (VNIR) spectral band are commercially available in sizes of several tens of millions of pixels. However, these commercially available FPAs are not yet available at frame rates above 1 to 2 per second and with electronic shuttering, which is needed for long-duration, persistent surveillance applications. The sizes of IR FPAs for day and night usage significantly lag behind sizes available in the VNIR. Progress in large IR FPAs has been made primarily in the MWIR band. Prior to DB-WAPSS, the largest IR FPA available was the 4-megapixel MWIR array, developed by NRL and L3 Communications, Cincinnati Electronics, Inc. (L3 CE), used on the Navy's SHARP system and for early persistent surveillance demonstrations.[1] Use of a reticulating process by L3 CE on the SHARP FPA design allowed scaling up in size from a 4-megapixel, 25-μm pixel pitch to a 16-megapixel, 15-μm pitch FPA on an only modestly larger die size than for the SHARP FPA. Further scale-up to 64 megapixels should be possible and is presently being explored.

The IR FPA is integrated into an IR Imaging Module (IRIM) that produces the high-speed output data. Non-uniformity corrections (NUC) and bad pixel replacement are calculated within the IRIM and applied in real time. The IRIM is preloaded with two preset integration times that correspond directly to two operating temperature ranges. The temperature ranges are operator selectable and can be used for either change in climate or change between day and night operation. The image data is output over four 14-bit CameraLink data ports, which are then converted by a multiplexer into two gigabit Ethernet outputs for interface convenience.

The VNIR capability of the DB-WAPSS 59/16 is provided by a ruggedized 59-megapixel CMOS camera, the V59M, produced by Teledyne Imaging Sensors. The camera produces a square-format of 7680 × 7680 pixels, and images at almost 10 frames per second (fps) with an electronic global shutter. The camera's high quality EO lens matches the same 22.8° field of view as the MWIR channel. The V59 output is also CameraLink, with possible conversion into multichannel gigabit Ethernet.

The IRIM and the V59 are integrated into a single unit and installed into a stabilized CA-247 gimbal. The sensor may be operated in IR, visible, or simultaneous EO/IR modes, gaining the benefits of fused multiband image products. Figure 7 shows the DB-WAPSS-59/16 sensor. The central rectangular box contains the IRIM, which uses the 16.7-megapixel MWIR FPA and the V59M camera with the 59-megapixel FPA. Large drive motors power both the roll and azimuth axes in the DB-WAPSS 59/16, allowing the sensor to slew quickly in large steps to commanded positions. The sensor is

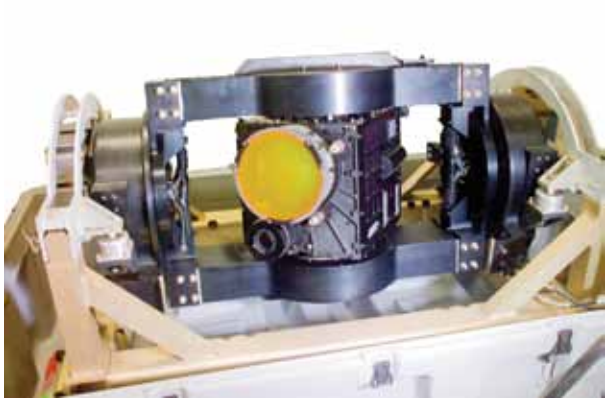

FIGURE 7
DB-WAPSS 59/16 camera. IR optics shown with yellow protective cover. VNIR optics below and to the left of the IR optics.

capable of stepping a 2 × 2 pattern of images in less than a second, maintaining a high degree of stabilization during frame exposures, and covering a total field of regard of approximately 36° on each side. The sensor is 40 in. long and has a rotational "keep-out" diameter (including sway space) of 24.75 in. If step-stare is not used, the imaging unit can frame faster than the 4-fps limit set by the stepping motors.

The sensor is designed to operate in harsh military environments on either manned or unmanned platforms. System mean-time-between-failure (MTBF) is estimated at greater than 2800 hours using MIL-HDBK-217.

Test and Evaluation: Seven 16.7-megapixel IRIM units were produced for Blue Devil DB-WAPSS sensors. Measured IRIM characteristics for five IRIMs are summarized in Table 1.

TABLE 1 — Measured IRIM Characteristics

Parameter	Average of 5 Units
Operability	99.0%
Max Power during Cool Down (W)	175.42
SS Power Operating at Temp. (W)	59
Weight (lb)	28

Sensor imaging performance was validated during factory test by measuring the system relative edge response (RER) and calculating the associated system modulation transfer function (MTF). Measured response has matched very closely with predicted performance from modeling. The production sensors have produced system RERs from 0.63 to 0.68, resulting in average system MTF values from 33% to 35% at the Nyquist frequency (33.3 lines/mm). Imagery captured during NRL flight tests show image quality commensurate with system MTF values in this range (Fig. 8).

Processing DB-WAPSS Sensor Data: DB-WAPSS sensor data were processed using NRL's "Blackjack" software suite designed for persistent surveillance applications. This software suite is based on the common open-architecture, standards-based design that NRL has used on many ISR data exploitation and fusion stations.[2] Blackjack satisfies two key processing requirements for DB-WAPSS: (a) processing at the full dynamic range of the raw camera outputs — 14-bits for the IRIM and 12-bits for the V59M, and (b) real-time processing and display for image formation and for target detection, identification, and tracking — without sacrificing full-dynamic range processing.

FIGURE 8
DB-WAPSS daytime MWIR flight imagery (June 9, 2009). Inset images show (top) a resolution target, and (bottom) vehicles in a magnified view of the parking area.

IR data from NRL flight tests have been processed to demonstrate the sensor's detection capability and its ability to detect subtle changes in revisited scenes and in tracking moving vehicles from an orbiting aircraft. The sensor's image stream, motion-video at 4 fps, was used to obtain the tracking results shown in Fig. 9. The imagery was of sufficient quality to implement an NRL motion-tracking algorithm that can reliably initiate and maintain tracks of moving targets under stressful conditions. The tracking algorithms executed on the processing system reliably reject false track initiations caused by parallax, and provide capability to track through temporary obscurations and momentary stoppage of movement. The high-quality MWIR image data complement the performance of the tracking system.

Summary: An advanced dual-band step-stare sensor using a 16.7-megapixel MWIR and a 59-megapixel

FIGURE 9
Top: Track initiations, indicated by green markers. Bottom: Track generation for three vehicles, T:1, T:2, and T:3.

visible array has been developed, and seven copies of the sensor constructed and tested for the Marine Corps' Angel Fire program and transitioned to the Air Force's Blue Devil program. Test results from these sensors demonstrated the reproducibility of the mechanical, data-handling, and high-quality MWIR-imaging performance. Airborne flights demonstrated a TRL-7 level of maturity. The quality of the MWIR data, together with NRL's real-time, standards-based processing, enables effective day/night change-detection and tracking performance.

Acknowledgments: The authors acknowledge the hard work of contributors at L3 Cincinnati Electronics, Goodrich ISR Barrington, and NRL, as well as staff members from Global Strategies, Inc., Smart Logic, Inc., Space Dynamics Laboratory, and Alaire Technologies, Inc., who worked closely with the NRL personnel throughout the program and contributed equally to its success. Specific contributions from Steve Frawley, Myra Lau, Don Thornburg, Kenneth Reese, Jason Edelberg, and Ralph York were invaluable during our flight test efforts.

[Sponsored by ONR, USMC, and the Joint IED Defeat Organization]

References

[1] J.N. Lee, J.G. Howard, M.R. Kruer, D.C. Linne von Berg, M. Colbert, S. Frawley, and M. Schicker, "Infrared Airborne Pod for Wide Area Day-Night Persistent Surveillance," invited presentation, 2005 National Military Sensing Symposium (MSS), Orlando, FL, Nov. 15, 2005.

[2] D. Linne von Berg, J.N. Lee, M. Kruer, M.D. Duncan, F.M. Olchowski, E. Allman, and G. Howard, "Airborne Net Centric Multi-INT Sensor Control, Display, Fusion, and Exploitation Systems," presented at Airborne Intelligence, Surveillance, Reconnaissance (ISR) Systems and Applications, SPIE Defense and Security Symposium, Orlando, FL, April 13, 2004, and published in *Proc. SPIE* **5409**, 111–119 (2004).